NASA Technical Memorandum 79131

THE FRICTION AND WEAR OF METALS AND BINARY ALLOYS IN CONTACT WITH AN ABRASIVE GRIT OF SINGLE-CRYSTAL SILICON CARBIDE

Kazuhisa Miyoshi and Donald H. Buckley
Lewis Research Center
Cleveland, Ohio

Prepared for the
Joint Lubrication Conference
cosponsored by the American Society of
Lubrication Engineers and the
American Society of Mechanical Engineers
Dayton, Ohio, October 16-18, 1979

1 Report No	2 Government Accession No	3 Recipient's Catalog No
NASA TM-79131		

4. Title and Subtitle	5. Report Date
THE FRICTION AND WEAR OF METALS AND BINARY ALLOYS IN CONTACT WITH AN ABRASIVE GRIT OF SINGLE-CRYSTAL SILICON CARBIDE	6. Performing Organization Code

7. Author(s)	8 Performing Organization Report No.
Kazuhisa Miyoshi and Donald H. Buckley	E-9973
	10. Work Unit No

9. Performing Organization Name and Address	11 Contract or Grant No
National Aeronautics and Space Administration Lewis Research Center Cleveland, Ohio 44135	

12 Sponsoring Agency Name and Address	13 Type of Report and Period Covered
National Aeronautics and Space Administration Washington, D.C. 20546	Technical Memorandum
	14 Sponsoring Agency Code

15 Supplementary Notes

16 Abstract

Sliding friction experiments were conducted with various metals and iron-base binary alloys (alloying elements Ti, Cr, Mn, Ni, Rh and W) in contact with single-crystal silicon carbide riders. Results indicate that the friction force in the plowing of metal and the groove height (corresponding to the wear volume of the groove) decrease linearly as the shear strength of the bulk metal increases. The coefficient of friction and groove height generally decrease, and the contact pressure increases with an increase in solute content of binary alloys. There appears to be very good correlation of the solute to iron atomic radius ratio with the decreasing rate of change of coefficient of friction, the decreasing rate of change of groove height and the increasing rate of change of contact pressure with increasing solute content. These rates of change increase as the solute to iron atomic radius ratio increases or decreases from unity.

17 Key Words (Suggested by Author(s))	18 Distribution Statement
Abrasive wear Silicon carbide Binary alloys Metals	Unclassified - unlimited STAR Category 26

19 Security Classif. (of this report)	20 Security Classif. (of this page)	21 No of Pages	22 Price*
Unclassified	Unclassified		

* For sale by the National Technical Information Service, Springfield, Virginia 22161

THE FRICTION AND WEAR OF METALS AND BINARY ALLOYS IN CONTACT WITH AN ABRASIVE GRIT OF SINGLE-CRYSTAL SILICON CARBIDE

by Kazuhisa Miyoshi and Donald H. Buckley

National Aeronautics and Space Administration
Lewis Research Center
Cleveland, Ohio 44135

E-9973

ABSTRACT

Sliding friction experiments were conducted with various metals and iron-base binary alloys (alloying elements Ti, Cr, Mn, Ni, Rh and W) in contact with single-crystal silicon carbide riders. Results indicate that the friction force in the plowing of metal and groove height (corresponding to the wear volume of the groove) decrease linearly as the shear strength of the bulk metal increases. The coefficient of friction and groove height generally decrease, and the contact pressure increases with an increase in solute content of binary alloys. There appears to be very good correlation of the solute to iron atomic radius ratio with the decreasing rate of change of coefficient of friction, the decreasing rate of change of groove height and the increasing rate of change of contact pressure with increasing solute content. These rates of change increase as the solute to iron atomic radius ratio increases or decreases from unity.

INTRODUCTION

Abrasive wear is the mechanism involved in the finishing of many surfaces. Filing, sanding, lapping, and grinding of surfaces all involve abrasive wear.

Khrushchov and Babichov (ref. 1) found that the resistance of metals to abrasive wear was related to their static hardness under two-body conditions; that is, it was inversely proportional to the Vickers hardness Hv of the initially annealed metal to a Vickers hardness of 430 (tungsten). Avient, Goddard, and Wilman (ref. 2) theoretically and experimentally indicate that the resistance of metals to abrasive wear was inversely proportional to the Vickers hardness of the fully work-hardened surface region on abraded metal at a Hv of about 250.

Similar results have been obtained by Rabinowicz, Dunn, and Russell (ref. 3) under three-body conditions. No attempt, however, has been made to explain in detail abrasive wear and friction in terms of the mechanical properties of metals such as shear strength. Further, there is a great lack of fundamental information relative to the friction energy dissipated in the abrasive wear processes. Such information can lead to reducing the energy consumed in such operations as grinding.

The objective of the present investigation was to examine the removal and plastic deformation of metal and the friction force in sliding contact with single-crystal silicon carbide abrasive grit as a function of metal properties such as shear strength. The investigation also examined the effect of alloying elements (Ti, Cr, Mn, Ni, Rh, and W) on the abrasive wear and friction behavior of several iron-base, binary solid-solution alloys. The riders of 0.025- and 0.040-millimeter-radius spherical silicon carbide were used to simulate abrasive grit. The sliding friction experiments were conducted with spherical riders sliding on the metal and alloy disks in mineral oil and in dry argon. Oil was used to minimize adhesion effects on friction. Single-pass sliding experiments were conducted with loads of 0.049 to 0.39 newton (5 to 40 g) at a sliding velocity of 3×10^{-3} meter/minute with a total sliding distance of 3 millimeters at room temperature.

SYMBOLS

A	projected area of contact, $\pi D^2/8$
C	solute content, at.%
D	width of a groove (wear track)
H	height of a groove (wear track)
H_v	Vickers hardness
$-dH/dC$	decreasing groove height with increasing C
dH_v/dC	alloy hardening rate with increasing C
K	solute to iron atomic radius ratio
k	constant for material
k'	constant for material
m	constant for material
n	constant for material (Meyer's index)
P	contact pressure during sliding, W/A

dP/dC	increasing contact pressure with increasing C
r	radius of spherical rider
W	normal load
μ	coefficient of friction
$-d\mu/dC$	decreasing coefficient of friction with increasing C

MATERIALS

The single-crystal silicon carbide used in these experiments was a 99.99-percent-pure compound of silicon and carbon and had a hexagonal-close-packed crystal structure, as indicated in table I.

The metals were all polycrystalline. The titanium was 99.97 percent pure, and the copper was 99.999 percent pure. All the other metals were 99.99 percent pure. Table II shows the crystalline, physical, and chemical properties of metal specimens.

Table III presents the analyzed compositions in atomic percent of iron-base binary alloys prepared by Stephens and Witzke (ref. 7). The iron-base binary alloys of reference 7 were prepared by arc-melting the high-purity iron and high-purity alloying elements (Ti, Cr, Mn, Ni, Rh, and W). The solute concentrations ranged from approximately 0.5 atomic percent for those elements that have extremely limited solubility in iron up to approximately 16 atomic percent for those elements that form a continuous series of solid solutions with iron.

EXPERIMENTAL APPARATUS AND PROCEDURE

Apparatus

The apparatus used in this investigation was a system capable of applying load and measuring friction in argon at atmospheric pressure and in oil. The mechanism for measuring friction is shown schematically and is described in reference 9.

Specimen Preparation

The surfaces of the single-crystal silicon carbide pin specimens (riders) were hemispherical and were polished with approximately 3-micrometer-diameter diamond powder and then 1-micrometer-diameter aluminum oxide (Al_2O_3) powder. The radii of curvature of the silicon carbide spherical riders

were 0.04 and 0.025 millimeter, as shown in figure 1. The orientations of the single-crystal silicon carbide riders are also shown in figure 1.

The surfaces of metal and iron-base binary alloy disk specimens were also polished with 3-micrometer-diameter diamond powder and then 1-micrometer-diameter aluminum oxide powder. Some of the alloy disk specimens were annealed under a vacuum of 10^{-4} to 10^{-5} pascal for 1 hour at the temperature where maximum solubility occurs in the α region. This anneal was followed by a 16 hour or more heating at 300° C in order to produce single-phase, homogenized, equiaxed, strain-free specimens (ref. 7).

Experimental Procedure

The silicon carbide, metal and alloy surfaces were rinsed with 200-proof ethyl alcohol before use. The friction experiments involved a single pass over a total sliding distance of 3 millimeters at a sliding velocity of 3 millimeters/minute and were conducted in dry argon (H_2O < 20 ppm) at atmospheric pressure and in degassed pure mineral oil. All experiments were conducted at room temperature.

RESULTS AND DISCUSSION

Friction and Wear Behaviors of Metals and Alloys

Sliding friction experiments were conducted with 0.04- and 0.025-millimeter-radius spherical silicon carbide riders in contact with disk surfaces of various metals and alloys in argon and in mineral oil. The friction-force traces obtained in this investigation are characterized by randomly fluctuating behavior, with no evidence of stick-slip (refs. 10 and 11). The sliding involves plastic flow and the generation of metal wear debris, the typical examples of which are shown in figures 2 and 3. Figure 2 shows a typical scanning electron micrograph and surface profile of a wear trace (groove) on an iron surface after sliding of a silicon carbide rider. (Surface profiles were recorded by a surface profilometer.) Figure 2 reveals that the sliding action resulted in a permanent groove in the metal surface, with considerable amount of deformed metal piled up along the sides of the groove. More detailed examination of this groove revealed further evidence of metal wear debris, as shown in figure 3. The wear debris particles are generated primarily on the sides of the wear track. Moreover, examination of the surface of the silicon carbide rider revealed transferred metal wear particles, as shown in figure 3(b). Figure 3(b) shows a scanning electron micrograph of the surface of the spherical silicon carbide rider at its tip, after

it had slid on an iron surface. The X-ray energy dispersive analysis for iron on the silicon carbide surface presented the evidence of the iron wear particles.

Thus, the foregoing typical results reveal that both plastic deformation and the generation of wear debris of metal occur as a result of sliding friction between a spherical silicon carbide rider and a metal surface. The amount of metal or alloy removed, however, was very much less than the volume of the groove (wear track) plowed out by the silicon carbide rider. Avient, et al., (ref. 2) indicate that abrasion on dry emery leads to an amount of wear (metal removal) corresponding to only about 10 percent of the volume of the grooves plowed out by the abrasives.

The width D and height H of a groove (wear track width and height) are defined in figure 2(b). The height H and width D of the grooves reported herein were obtained by average measurements of 8 to 10 surface-profile traces. Contact pressure P during sliding may, then, be defined by $P = W/A$, where W is the applied normal load and A is the projected area of contact and is given by $A = \pi D^2/8$ (only the front half of the rider is in contact with the flat specimen). The relation between the groove widths D generated by the rider and the load W would be expressed by $W = kD^n$, which is known as Meyer's law (ref. .10). The value of n as determined for cubic and hexagonal metals lies between 2.0 and 2.2, except for titanium and zirconium. With titanium and zirconium, n is near 2.8. The n-value of titanium and zirconium might differ from those of other hexagonal metals because titanium and zirconium do not slip predominantly on the basal planes (slip plane, $\langle 0001 \rangle$; slip direction, $\langle 11\bar{2}0 \rangle$ such as do the metals magnesium, cobalt, and rhenium. Titanium and zirconium slip predominantly on the prismatic planes (slip plane; $\langle 10\bar{1}0 \rangle$, slip direction; $\langle 11\bar{2}0 \rangle$) during plastic deformation. The relation between the groove height H and the load W could be expressed by $W = k'H^m$, where k' and m were constants for the metal under examination. The value of m for cubic and hexagonal metals lies between 1.1 and 1.2.

Effects of Shear Strength of Metals

In argon. - Figure 4 presents the coefficients of friction and the groove heights for various metals after sliding experiments at a load of 20 grams in argon at atmospheric pressure. There is no obvious correlation between coefficient of friction and contact pressure ($P = W/A$), which depends on the metal properties. The relationship between groove height and contact pressure is a nearly linearly decreasing one, but the rate of decrease (slope) changes at a contact pressure of about 230 kilogram/square millimeter. The relationship between

the inverse of the groove height is a nearly proportional to the contact pressure, but the slope changes at a contact pressure of about 320 kilogram/square millimeter. The relationship between the inverse of the groove height and the contact pressure is comparable to these obtained by Avient, Goddard, and Wilman (ref. 2) for various metals initially wet abraded on no. 3 emery paper and then slid under a 2.9-newton (300-g) load on dry grade no. 3 emery paper (particles of 150-μm mean diameter). Avient, et al., established that, for Vickers hardness (Hv) of the abraded metal to about 250, the inverse of the abrasive wear rate is approximately proportional to Hv but that the mean locus appears to curve upward away from the Hv axis at higher Hv. Thus, the results of figure 4 are similar to those obtained by Avient, et al., (ref. 2) in the full-scale wear test.

The stress in the metal, applied to only a very small area of the contacting surface, is evidently complicated. Therefore, the shear and flow properties of the metal in the abrasive wear processes have been indirectly expressed by various means and these include static Vickers hardness (refs. 1 and 2); scratch hardness (ref. 12); mean stress supporting load (ref. 13); contact pressure (fig. 4 and ref. 10); plowing stress (ref. 12); mean stress opposing sliding (ref. 13); and so on.

On the other hand, the anisotropics of deformation and friction of single crystals in the abrasive wear processes have been explained in terms of the distribution of resolved shear stresses acting on the slip system in crystals during sliding (ref. 14). The concept of shear stress, however, has been only slightly related to the abrasive, friction, and wear properties of polycrystalline metals because the mechanism of deformation for the polycrystalline case is quite complicated.

The ultimate shear strength of a metal is very strongly dependent on the mean contact pressure (ref. 15 or ref. 10), generally increasing with increased applied hydrostatic pressure.

Figure 5 presents the coefficients of friction and groove heights for various metals as a function of shear strength. The shear strength was estimated from the contact pressure data in figure 4 by using the relation between hydrostatic pressure and shear strength in reference 15. The relation between the groove height and the shear strength of the metal shows that H decreases linearly with shear strength, except for molybdenum and tungsten, which have the highest shear strengths. The exceptions of molybdenum and tungsten arise from the geometry of the rider and the load. This matter will be discussed in the later section. The coefficient of friction in figure 5 may be governed by two factors: (1) shearing at the interface and (2) plowing in the metal. The shearing force at the interface in dry friction is comparable in magnitude to the plowing force in the metal and depends on the nature of the interface.

It is, therefore, anticipated that there is no obvious relationship between coefficient of friction and contact pressure in figure 5 because the coefficient of friction is strongly influenced by variations of shearing force at the interface. This subject is discussed more fully in succeeding sections.

The present authors have conducted sliding friction experiments to determine shearing friction at the interface with spherical metal riders in contact with disks of silicon carbide (0001) surfaces in both argon and in mineral oil (ref. 10). The experimental procedure and conditions were the same as those used herein. In argon the metal rider slid on the silicon carbide disk and shearing at the interface was primarily responsible for the friction behavior observed. The coefficients of friction in argon at atmospheric pressure were all less than 0.2. The metals exhibited a variation in friction, as anticipated.

The results of figure 5, in which the silicon carbide rider plowed a groove in the metal surface, revealed that shearing at the interface and plowing of the bulk metal are responsible for the friction behavior observed. The shearing force is approximately the same as the plowing force; this is arrived at by comparing the results of figure 5 with those of reference 10 except for magnesium, aluminum, and zirconium. Although the shearing force at the interface and the plowing force are usually separable, with magnesium, aluminum, and zirconium, shearing at the interface and plowing of the metal seem to interact and are not separable in figure 5.

On the other hand, the coefficients of friction in oil were all approximately 0.05. The variation in friction for various metals was negligibly small. It is, therefore, anticipated that sliding experiments in oil, in which a hard silicon carbide rider plows a groove in a metal surface, may reveal a relationship between the coefficient of friction and a property of the bulk metal such as shear strength.

In oil. - Sliding friction experiments were conducted with the 0.04-millimeter-radius spherical silicon carbide rider in contact with surfaces of various metal disks in mineral oil. Figure 6 shows the coefficient of friction and the groove height for various metals at a load of 20 grams. In figures 6(a) and (b), the coefficient of friction and the groove height correlate with the shear strength of the metal, except for molybdenum and tungsten, as might be anticipated from figure 5. The relationship between the coefficient of friction and the shear strength is a linearly decreasing one as is the relationship between groove height and shear strength. Figure 6(c) presents the relationship between the contact pressure during sliding and the shear strength estimated from the contact pressure data by using the relation between hydrostatic pressure and shear strength from reference 15. The contact pressure is approximately proportional to the shear strength. In the results in figure 6, however,

molybdenum and tungsten were exceptions. With these metals the grooves produced by plowing of the rider were the smallest for all the metals. There may be a lower limit to the validity of the correlation between the groove height and the shear strength. This lower limit seems to depend (1) on the geometry of the rider, that is, the radius of the spherical rider, and (2) on the load. A ratio of groove width to rider radius of about 0.25 may be the lower limit of the validity in figure 6.

Sliding friction experiments were also conducted with a spherical silicon carbide rider having a smaller radius (0.025 mm) in contact with a metal disk in mineral oil. The coefficients of friction, the groove heights and the contact pressures are presented as a function of shear strength in figure 7. Large grooves were produced in magnesium, aluminum, copper, zirconium, and iron. Experiments with these metals were therefore conducted at a load of 5 grams. Because relatively smaller grooves were produced in titanium, nickel, rhodium, molybdenum, and tungsten, experiments with these metals were conducted at a load of 20 grams.

In figure 7, the coefficient of friction and the groove height correlate with the shear strength of the metal, and the relationships are approximately linearly decreasing, without exception. In this experiment, the ratio of the groove width to the rider radius D/r ranged from about 0.36 to 0.5. Thus, the coefficient of friction, particularly the plowing term (in that coefficient), and the groove height corresponding to the groove volume may be governed by two factors: (1) the shear strength at the interface and (2) the shear strength of the bulk metal. In figure 7, the contact pressure is nearly proportional to the shear strength of the metal.

Alloying Element Effects

Sliding friction experiments were conducted with 0.025-millimeter-radius, spherical, single-crystal silicon carbide riders in contact with surfaces of various iron-base alloys in mineral oil. The binary-alloy systems were iron alloyed with titanium, chromium, manganese, nickel, rhodium, or tungsten.

The coefficients of friction and the groove height (corresponding to the volume of the groove) for a number of binary alloys are presented in figures 8 and 9 as functions of solute content (atomic percent) at loads of 0.05 and 0.1 newton. The data of these figures indicate decreases in the coefficient of friction and groove height with an increase in solute content. Examination of figures 8 and 9 show no significant change in coefficient of friction with load, but there are obvious differences in the groove height with load. The average rates of decrease in the coefficient of friction and the groove height strongly depend on the alloying element. This matter will be discussed in controlling

mechanisms of friction and wear.

Figure 10 presents the contact pressure during sliding for various binary alloys as a function of solute content (in atomic percent) at loads of 0.05 and 0.1 newton. The contact pressure increases as the solute content increases, and the increasing rate in contact pressure depends on the alloying element. There is no significant change in contact pressure with load. The contact pressure was calculated from the groove width.

Controlling Mechanisms of Friction and Wear

Alloy hardening at high temperatures (300 and 411 K) and alloy softening at lower temperatures (77 and 188 K) have been observed in several iron-base binary alloys by Leslie and Spitzig (refs. 16 and 17), Pink (ref. 18), Leemans and Fine (ref. 19), and Stephens and Witzke (ref. 4). These investigations concluded that for many alloy systems both alloy softening and alloy hardening were controlled by atomic size misfit or the solute iron atomic radius ratio.

The grooves in this investigation (wear tracks) were formed in the alloys primarily by the mechanism of plastic deformation (under hydrostatic contact pressure) and the plowing stress associated with sliding. In addition there was occasional material removal, as already mentioned.

The formation of grooves may be very similar to that of hardness test indentations. Therefore, the manner in which the friction and wear properties correlate with the solute to iron atomic radius ratio or atomic size misfit is of interest. Figure 11 presents the decreasing rates of coefficient of friction $-d\mu/dC$ and groove height $-dH/dC$, and the increasing rate of contact pressure dP/dC with an increase of solute contents as a function of solute to iron atomic radius ratio at loads of 0.1 and 0.05 newton. The rates were estimated from the data in figures 8 to 10.

There appears to be very good agreement between the friction and wear properties, and the solute to iron atomic radius ratio. The correlation between each rate and the solute to iron atomic radius ratio is separated into two cases: first, the case for alloying with manganese and nickel, which have smaller atomic radii than iron, and second, the case for chromium, rhodium, tungsten, and titanium, which have larger atomic radii than iron. The $-d\mu/dC$, $-dH/dC$, and dP/dC increase as the solute to iron atomic radius ratio increases or decreases from unity. Thus, the correlations indicate that atomic size of the solute is an important parameter in controlling abrasive wear, and friction in iron-base, binary alloys as well as alloy hardening reported by Stephens and Witzke (see fig. 11(c) and ref. 7).

Leslie concluded in his review that the atomic size misfit parameter is a reasonably good indicator of the strengthening of α-iron by the addition of low concentrations of substitutional solutes (ref. 16). The present authors have already shown that the abrasive wear and friction are strongly related to the shear strength of the pure metals. These two conclusions suggest that abrasive wear and friction can be correlated with atomic size misfit and shear strength in alloys and metals.

Deformation Effects of Mechanical Polishing

Because of concern for mechanical polishing effects on abrasive wear, this effect was examined. Sliding friction experiments were conducted with 0.025 millimeter-radius, spherical silicon carbide riders in contact with both annealed and mechanically polished iron-titanium binary alloy disk surfaces in mineral oil at loads of 0.05, 0.1, and 0.2 newton (ref. 11). The coefficient of friction and groove height generally decrease as the titanium content increases. The contact pressure (corresponding to the microhardness) increases with increases in the titanium content. The decreasing rates of both the coefficient of friction and the groove height and the increasing rates of the contact pressure are larger for the annealed surfaces than for mechanically polished surfaces. The trends of the data, however, for both the annealed and polished surfaces are similar.

CONCLUSIONS

As a result of sliding friction experiments conducted with spherical single-crystal silicon carbide riders in sliding contact with various metals, the following conclusions were drawn:

1. Both the friction force in the plowing of the metal and the groove height corresponding to the groove volume are related to the shear strength of the metal; that is, they decrease linearly with the ultimate shear strength of the bulk metal.

2. The atomic size and content of alloying element play a dominant role in controlling the abrasive wear and friction properties of binary, iron-base alloys.

3. The coefficient of friction and groove height (wear volume) generally decrease, and the contact pressure increases with an increase in solute content C.

4. There appears to be very good agreement between the decreasing rate of coefficient of friction $-d\mu/dC$, the decreasing rate of groove height (wear volume) $-dH/dC$, and the increasing rate of contact pressure dP/dC with an

increase of solute content C and the solute to iron atomic radius ratio. Those rates increase as the solute to iron atomic radius ratio increases or decreases from unity.

REFERENCES

1. Krushchov, M. M. and Babichev, M. A., "Resistance to Abrasive Wear and Elasticity Modulus of Metals and Alloys," Soviet Physics-Doklady, Vol. 5, 1960-1961, pp. 410-412.

2. Avient, B. W. E., Goddard, J.; and Wilman, H., "An Experimental Study of Friction and Wear During Abrasion of Metals," Proceedings of the Royal Society of London, Series A, Vol. 258, No. 1293, 18 Oct. 1960, pp. 159-180.

3. Rabinowicz, E., Dunn, L. A., and Russell, P. G., "A Study of Abrasive Wear Under Three-Body Conditions," Wear, Vol. 4, 1961, pp. 345-355.

4. Shaffer, P. T. B., "Effect of Crystal Orientation on Hardness of Silicon Carbide," Journal of the American Ceramic Society, Vol. 47, No. 9, Sep. 1964, p. 466.

5. Barrett, C. S., Structure of Metals, Crystallographic Methods, Principles, and Data, McGraw-Hill, New York, 1943, pp. 552-554.

6. Gschneidner, K. A., Jr., "Physical Properties and Interrelationships of Metallic and Semimetallic Elements," Solid State Physics, Vol. 16, F. Seitz and D. Turnbull, eds., Academic Press, 1965, pp. 275-426.

7. Stephens, J. R. and Witzke, W. R., "Alloy Softening in Binary Iron Solid Solutions," Journal of the Less-Common Metals, Vol. 48, Aug. 1976, pp. 285-308.

8. Hume-Rothery, W. and Raynor, G. V., The Structure of Metals and Alloys, 4th ed., The Institute of Metals; London, 1962, pp. 246-258.

9. Miyoshi, K. and Buckley, D. H., "Friction, Deformation and Fracture of Single-Crystal Silicon Carbide," American Society of Lubrication Engineers Transactions, Vol. 22, No. 1, 1979, pp. 79-90.

10. Miyoshi, K. and Buckley, D. H., "Friction and Wear of Metals with a Single-Crystal Abrasive Grit of Silicon Carbide - Effect of Shear Strength of Metal," NASA TP-1293, 1978.

11. Miyoshi, K. and Buckley, D. H., "Friction and Wear with a Single-Crystal Abrasive Grit of Silicon Carbide in Contact With Iron-Base Binary Alloys in Oil - Effects of Alloying Element and Its Content," NASA TP-1394, 1979.

12. Gane, N. and Skinner, J., "The Friction and Scratch Deformation of Metals on a Micro Scale," Wear, Vol. 24, 1973, pp. 207-217.

13. Childs, T. H. C., "The Sliding of Rigid Cones Over Metals in High Adhesion Conditions," International Journal of Mechanical Sciences, Vol. 12, 1970, pp. 393-403.

14. Bowden, F. P. and Brookes, C. A., "Frictional Anisotropy in Nonmetallic Crystals," Proceedings of the Royal Society of London, Series A, Vol. 295, No. 1442, Dec. 1966, pp. 244-258.

15. Bridgman, P. W., "Shearing Phenomena at High Pressures, Particularly in Inorganic Compounds," Proceedings of the American Academy of Arts and Sciences, Vol. 71, 1937, pp. 387-460.

16. Leslie, W. C., "Iron and Its Dilute Substitutional Solid Solutions," Metallurgical Transactions, Vol. 3, Jan. 1972, pp. 5-26.

17. Spitzig, W. A. and Leslie, W. C., "Solid-Solution Softening and Thermally Activated Flow in Alloys of Fe with Three Atomic Percent Co, Ni, or Si. Acta Metallurgica, Vol. 19, No. 11, 1971, pp. 1143-1152.

18. Pink, E., "Legierungsentfestigung in kubisch-raumzentrierten Meallen (Alloy Softening in Body Centered Cubic Metals)," Zeitschrift fuer Metallkunde, Vol. 64, No. 12, 1973, pp. 871-881.

19. Leemans, D. and Fine, M. E., "Solid Solution Softening and Strain-Rate Sensitivity of Fe-Re and Fe-Mo Alloys," Metallurgical Transactions, Vol. 5, No. 6, 1974, pp. 1331-1336.

TABLE I. - COMPOSITION DATA, CRYSTAL STRUCTURE, AND HARDNESS OF SINGLE-CRYSTAL SILICON CARBIDE

(a) Composition[a]

Si	C	O	B	P	Others
66.6%	33.3%	<500 ppm	<100 ppm	<200 ppm	<0.1 ppm

(b) Structure

Interatomic distance		Lattice ratio, c/a
a	c	
3.0817	15.1183	4.9058
3.073	15.079	4.9069

(c) Hardness data[b]

Plane	Direction	Knoop hardness number
(0001)	$\langle 11\bar{2}0 \rangle$	2917
(0001)	$\langle 10\bar{1}0 \rangle$	2954
$(10\bar{1}0)$	$\langle 0001 \rangle$	2129
$(10\bar{1}0)$	$c_{\perp}\langle 0001 \rangle$	27.55
$(11\bar{2}0)$	$\langle 0001 \rangle$	2391
$(11\bar{2}0)$	$c_{\perp}\langle 0001 \rangle$	2755

[a]Manufacturer's analyses.
[b]Ref. 4.
[c]Perpendicular to the $\langle 0001 \rangle$.

E-9973

TABLE II. - CRYSTALLINE, PHYSICAL, AND CHEMICAL PROPERTIES OF METALS

Metal	Purity, percent (a)	Crystal structure at 25° C (b)	Lattice constant, Å (10^{-10} m) (b)	Cohesive energy (c)		Shear modulus (c)	
				J/(g)(atom)	kcal/(g)(atom)	Pa	kg/cm^2
Iron	99.99	Body-centered cubic	a = 2.8610	416×10^3	99.4	8.15×10^{10}	$0.831\pm0.006\times10^{-6}$
Chromium		↓	a = 2.8786	395	94.5	11.7	1.19
Molybdenum		↓	a = 3.1403	657.3	157.1	11.6	1.18
Tungsten		↓	a = 3.1586	835.5	199.7	15.3	1.56±0.04
Aluminum		Face-centered cubic	a = 4.0414	322	76.9	2.66	0.271±0.001
Copper	99.999	↓	a = 3.6080	338	80.8	4.51	0.460±0.015
Nickel	99.99	↓	a = 3.5169	428.0	102.3	7.50	0.765
Rhodium		↓	a = 3.7956	556.5	133.0	14.7	1.50±0.03
Magnesium		Hexagonal close-packed	a = 3.2022	148	35.3	1.74	0.177
		↓	c = 5.1991				
Zirconium		↓	a = 3.223	609.6	145.7	3.41	0.348±0.008
		↓	c = 5.123				
Cobalt		↓	a = 2.507	425.5	101.7	7.64	0.779
		↓	c = 4.072				
Titanium	99.97	↓	a = 2.953	469.4	112.2	3.93	0.401±0.005
		↓	c = 4.729				
Rhenium	99.99	↓	a = 2.7553	779.1	186.2	17.9	1.82
		↓	c = 4.4493				

[a]Manufacturer's analysis.

[b]From ref. 5.

[c]From ref. 6.

TABLE III. - CHEMICAL ANALYSIS (REF. 7) AND SOLUTE TO IRON ATOMIC RADIUS RATIOS FOR IRON-BASE BINARY ALLOYS

Solute element	Analyzed solute content, at. %	Analyzed interstitial content, ppm by weight			Solute to iron atomic radius ratios (ref. 8)
		C	O	P	
Ti	1.02	56	92	7	1.1476
	2.08	--	---	--	↓
	3.86	87	94	9	
	8.12	--	---	--	
Cr	0.99	--	---	--	1.0063
	1.98	50	30	12	↓
	3.92	--	---	--	
	7.77	40	85	10	
	16.2	--	---	--	
Mn	0.49	--	---	--	0.9434
	.96	39	65	6	↓
	1.96	--	---	--	
	3.93	32	134	8	
	7.59	--	---	--	
Ni	0.51	--	---	--	0.9780
	1.03	28	90	6	↓
	2.10	--	---	--	
	4.02	48	24	5	
	8.02	--	---	--	
	15.7	38	49	7	
Rh	1.31	--	---	--	1.0557
	2.01	20	175	22	↓
	4.18	--	---	--	
	8.06	12	133	19	
W	0.83	30	140	12	1.1052
	1.32	--	---	--	↓
	3.46	23	61	21	
	6.66	--	---	--	

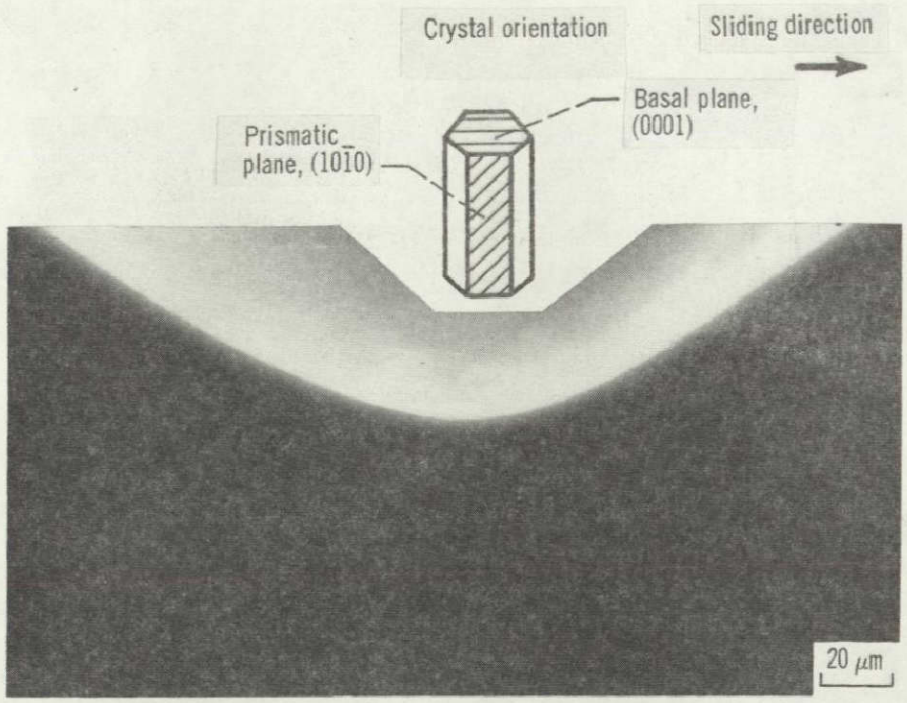

(a) 0.04-Millimeter-radius rider.

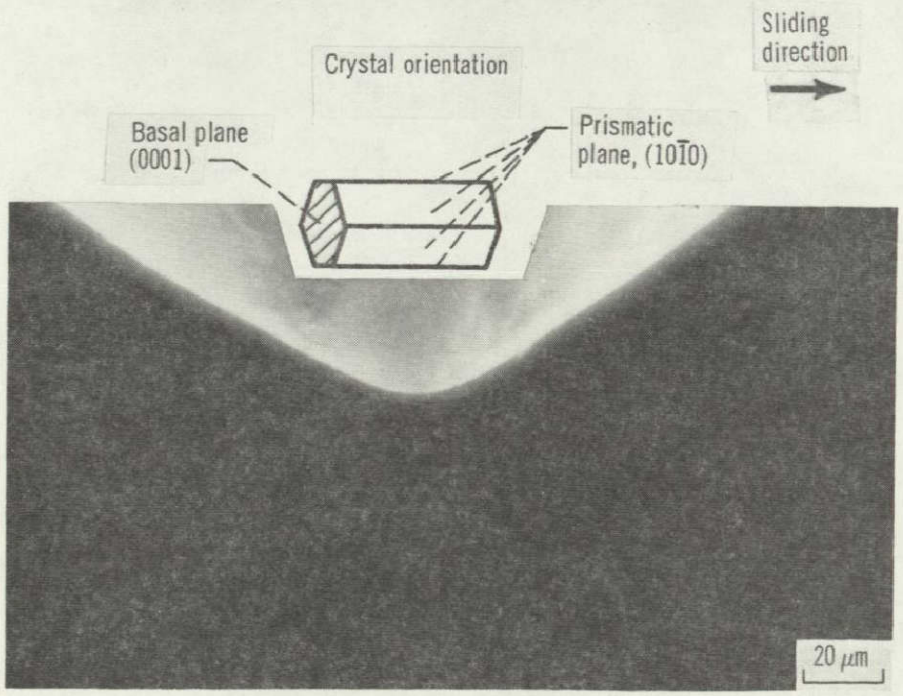

(b) 0.025-Millimeter-radius rider.

Figure 1. - Spherical silicon carbide riders.

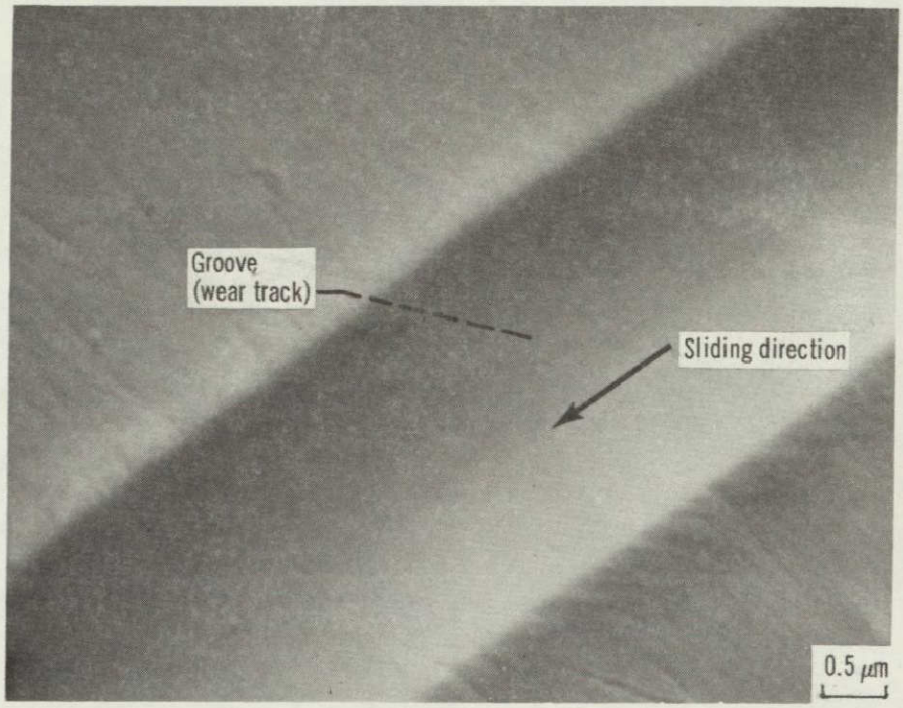

(a) Scanning electron micrograph.

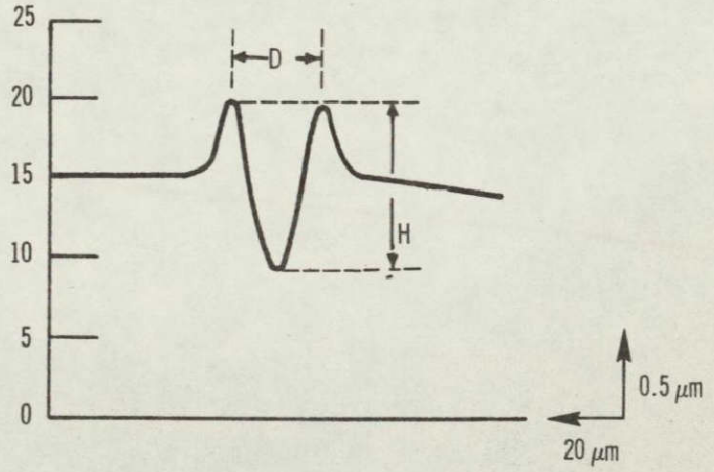

(b) Surface profile. Load, 30 grams.

Figure 2. - Groove on iron surface. Single-pass sliding of 0.04-millimeter-radius silicon carbide rider; sliding velocity, 3 mm/min; load, 30 grams (0.29 N); temperature, 25° C; environment, argon; pressure, atmospheric.

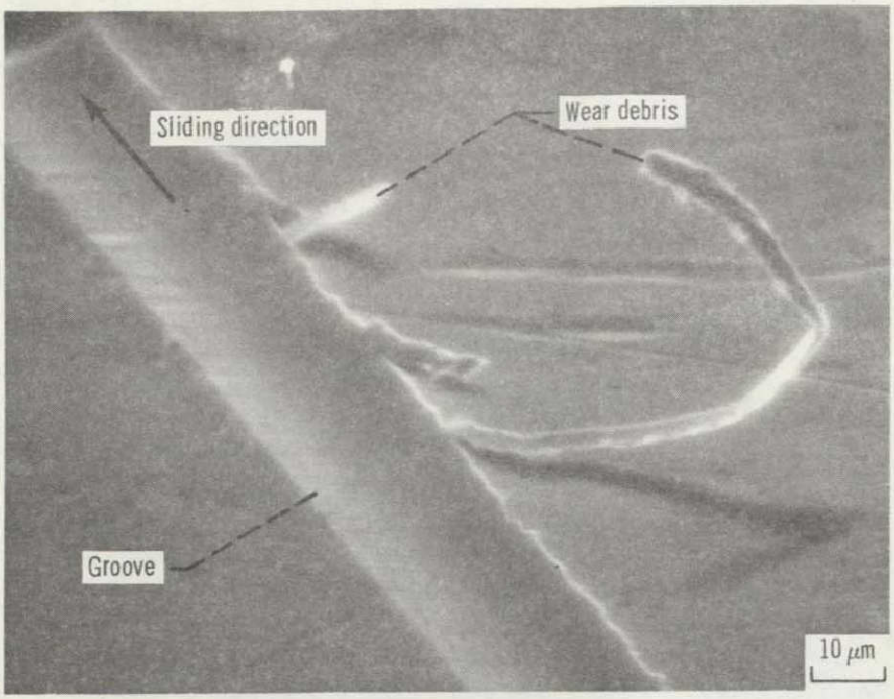

(a) Iron wear debris and groove on iron surface.

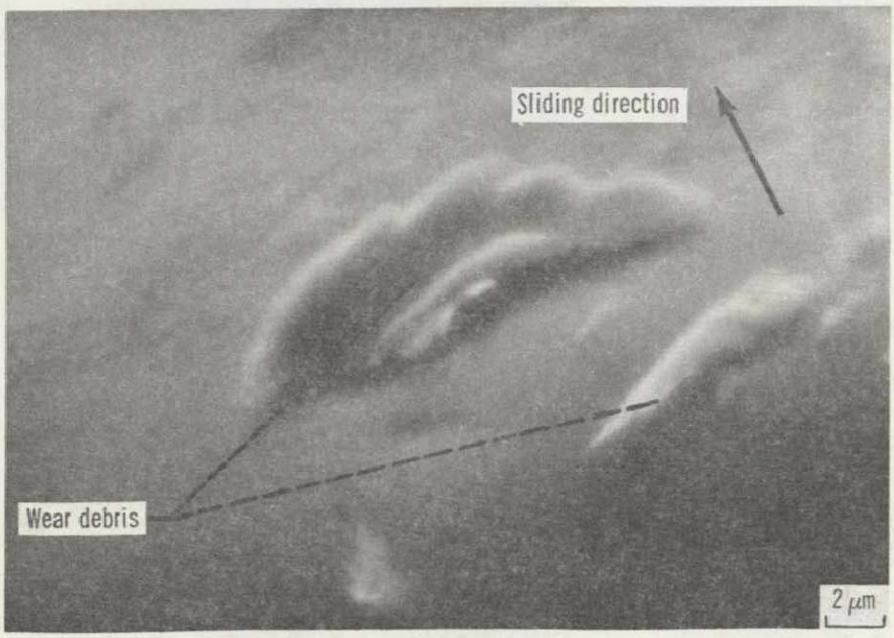

(b) Iron wear debris transferred to silicon carbide.

Figure 3. - Iron wear debris and groove. Single-pass sliding of 0.04-millimeter-radius silicon carbide rider; sliding velocity, 3 mm/min; load, 25 grams (0.25 N); temperature, 25° C; environment, argon; pressure, atmospheric.

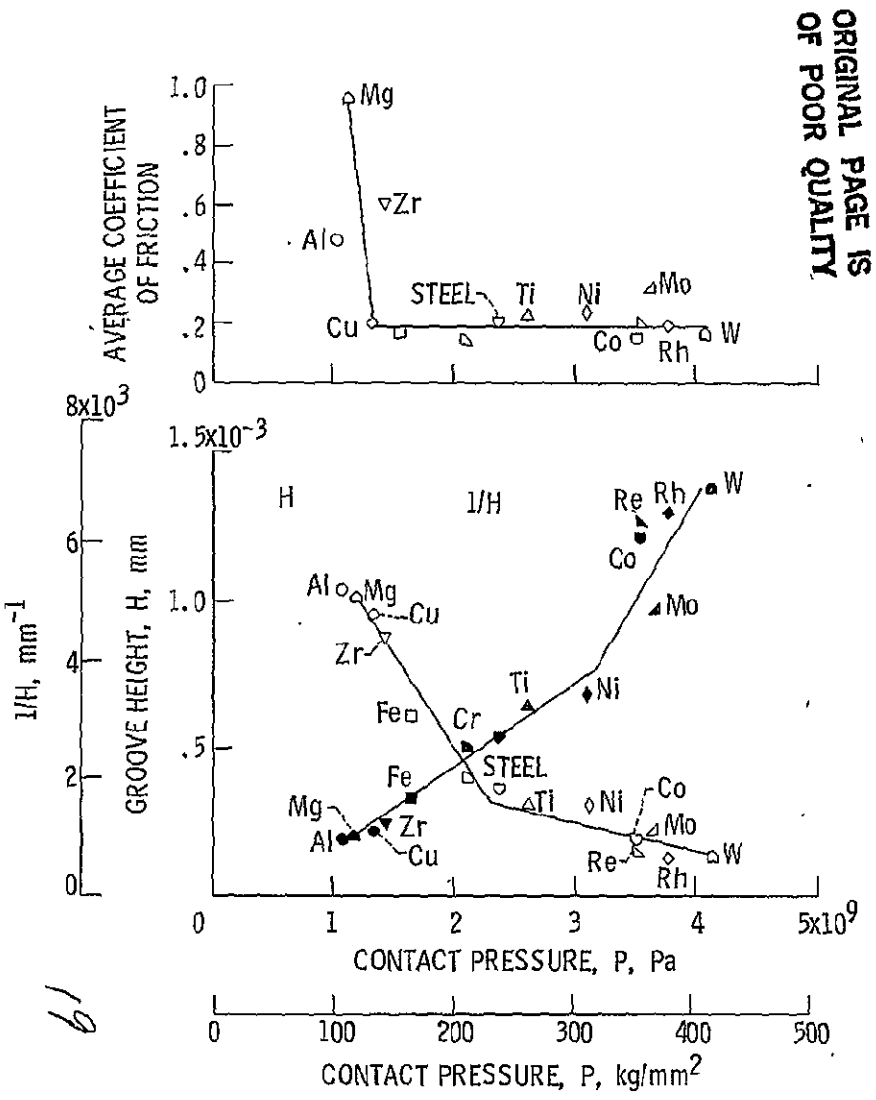

Figure 4. - Coefficient of friction and groove height as a function of contact pressure for various metals. Single-pass sliding of 0.04-millimeter-radius silicon carbide rider; sliding velocity, 3 mm/min; load, 20 grams; temperature, 25° C; environment, argon; pressure, atmospheric.

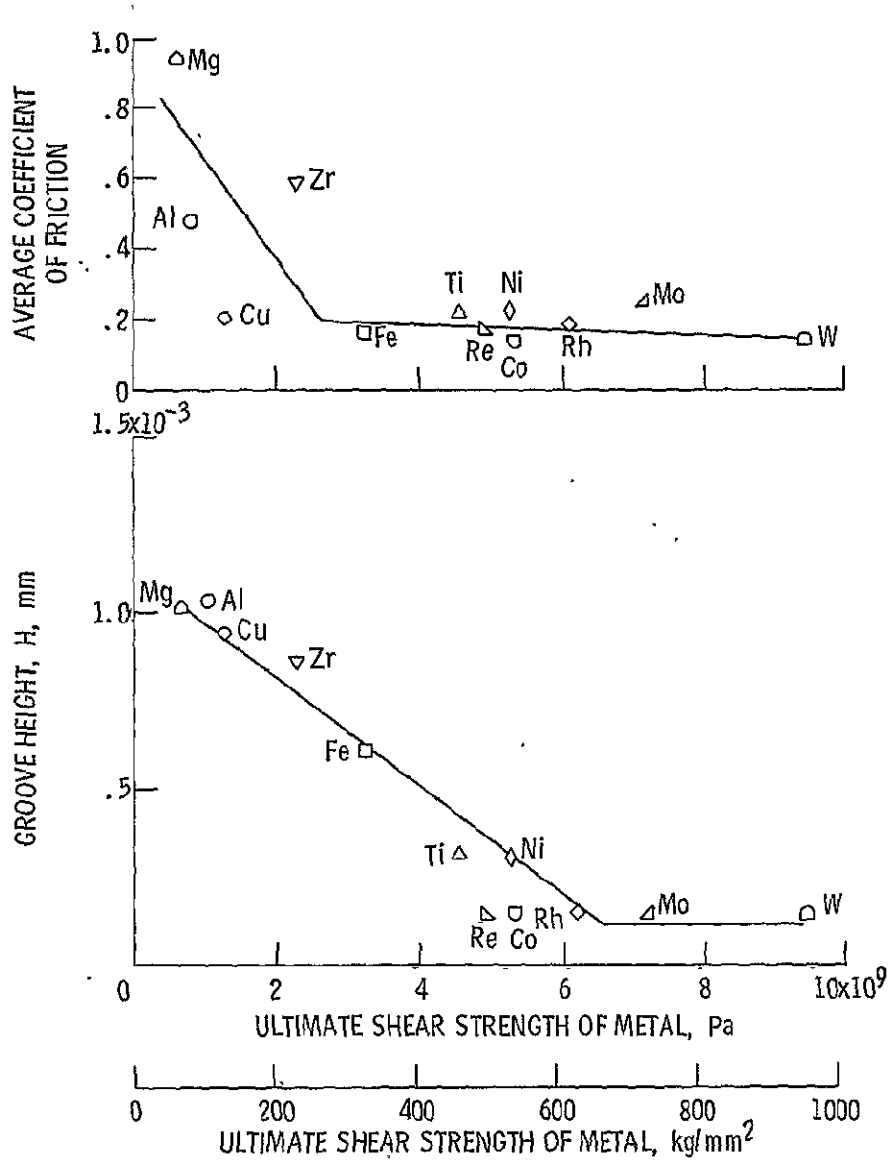

Figure 5. - Coefficient of friction and groove height as a function of shear strength for various metals. Single-pass sliding of 0.04-millimeter-radius silicon carbide rider; sliding velocity, 3 mm/min; load, 20 grams (0.2 N); temperature, 25° C; environment, argon; pressure, atmospheric.

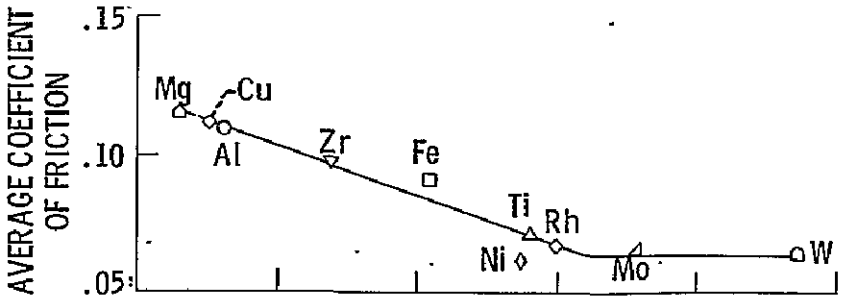

(a) AVERAGE COEFFICIENT OF FRICTION.

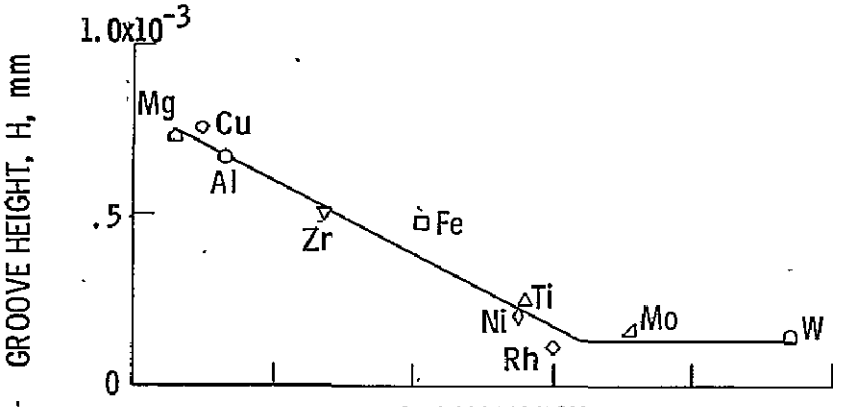

(b) GROOVE HEIGHT.

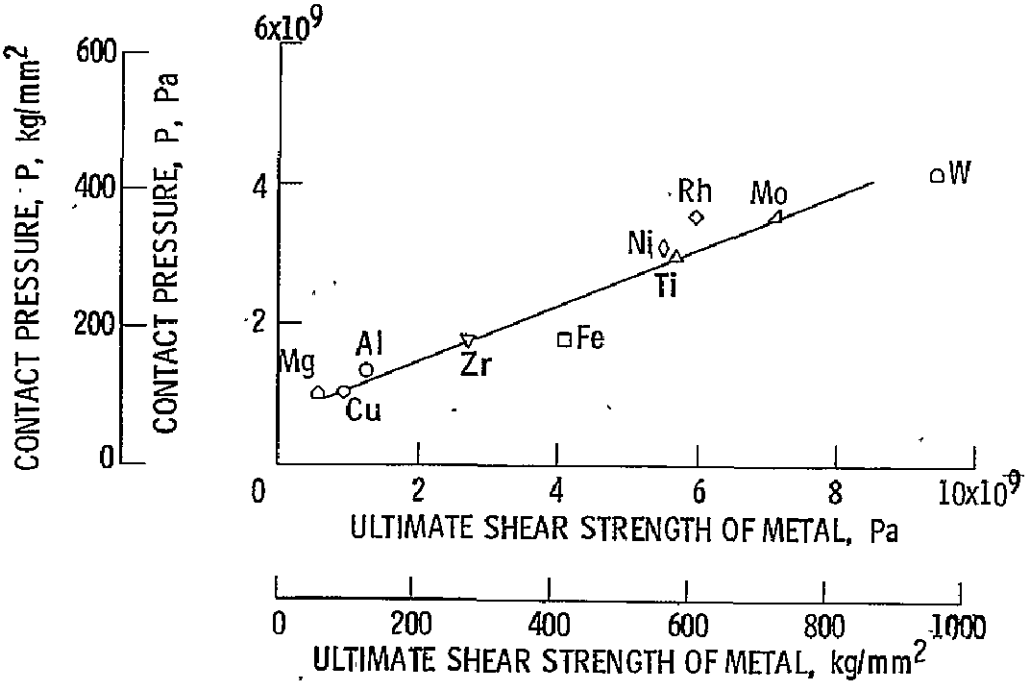

(c) CONTACT PRESSURE.

Figure 6. - Coefficient of friction, groove height, and contact pressure as a function of shear strength for various metals as a result of single-pass sliding of 0.04-millimeter-radius silicon carbide rider in mineral oil. Sliding velocity, 3 mm/min; load, 20 grams; temperature, 25° C.

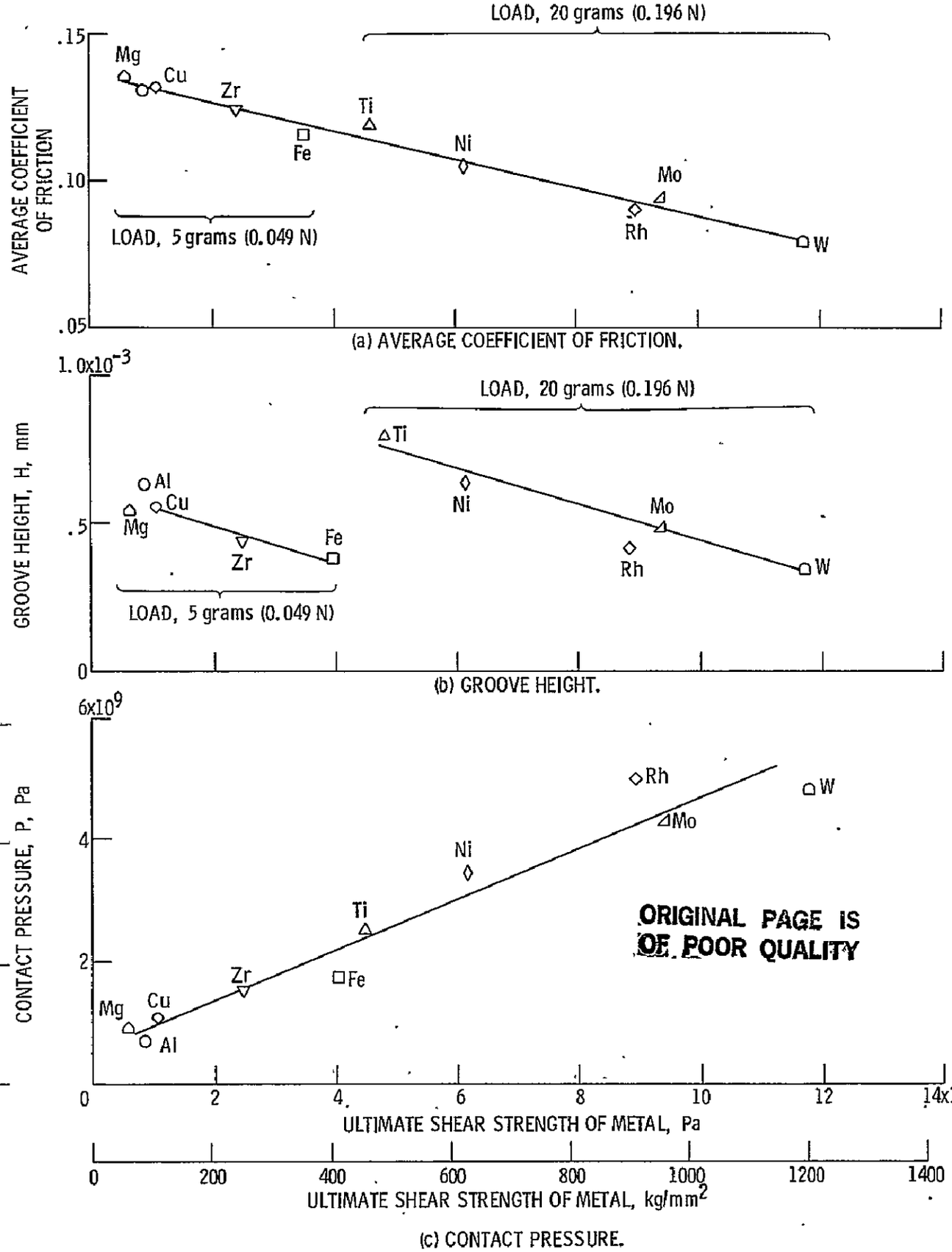

E-9973

Figure 7. - Coefficient of friction, groove height, and contact pressure as a function of shear strength for various metals as a result of single-pass sliding of 0.025-millimeter-radius silicon carbide rider in mineral oil. Sliding velocity, 3 mm/mm; load, 5 or 20 grams; temperature, 25° C.

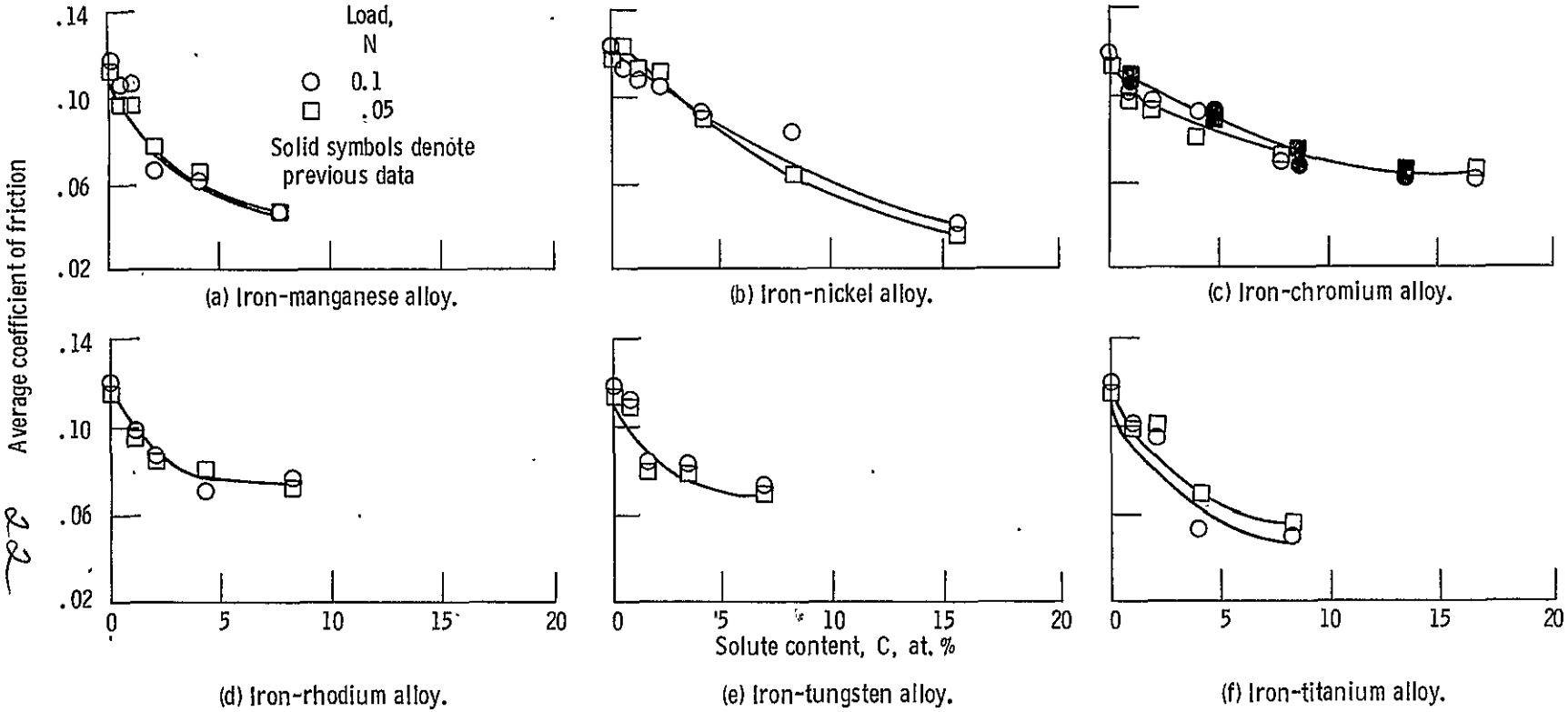

Figure 8. - Coefficients of friction for various iron-base alloys and pure iron as function of solute content. Single-pass sliding of 0.025-mm-rad. silicon carbide rider in mineral oil. Sliding velocity, 3 mm/min; temperature, 25^{0} C.

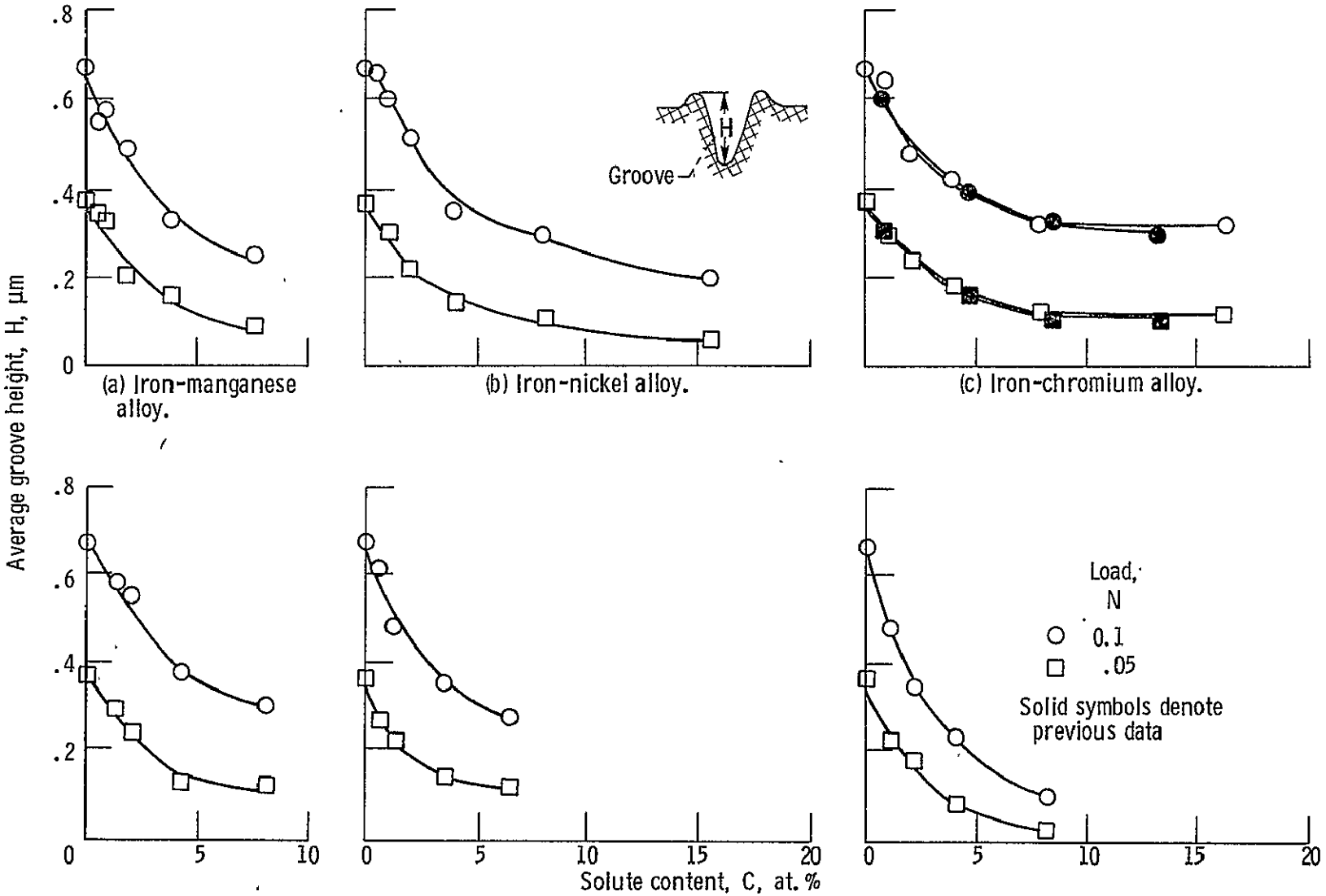

Figure 9. - Groove heights for various iron-base alloys and pure iron as function of solute content. Single-pass sliding of 0.025-mm-rad. silicon carbide rider in mineral oil. Sliding velocity, 3 mm/min; temperature, 25° C.

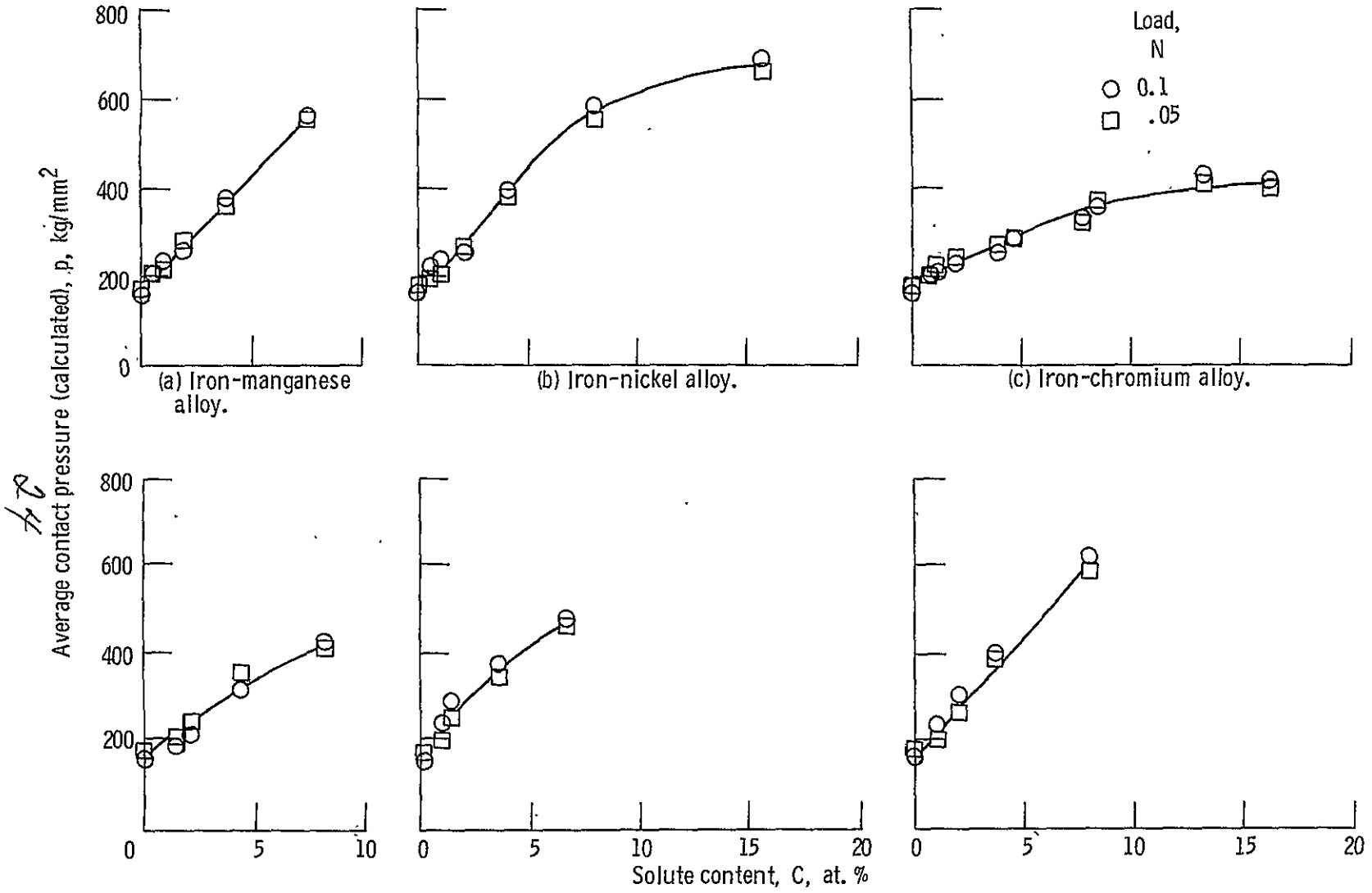

Figure 10. - Contact pressure for various iron-base alloys and pure iron as function of solute content. Single-pass sliding of 0.025-mm-rad. silicon carbide rider in mineral oil. Sliding velocity, 3 mm/min; temperature, 25° C.

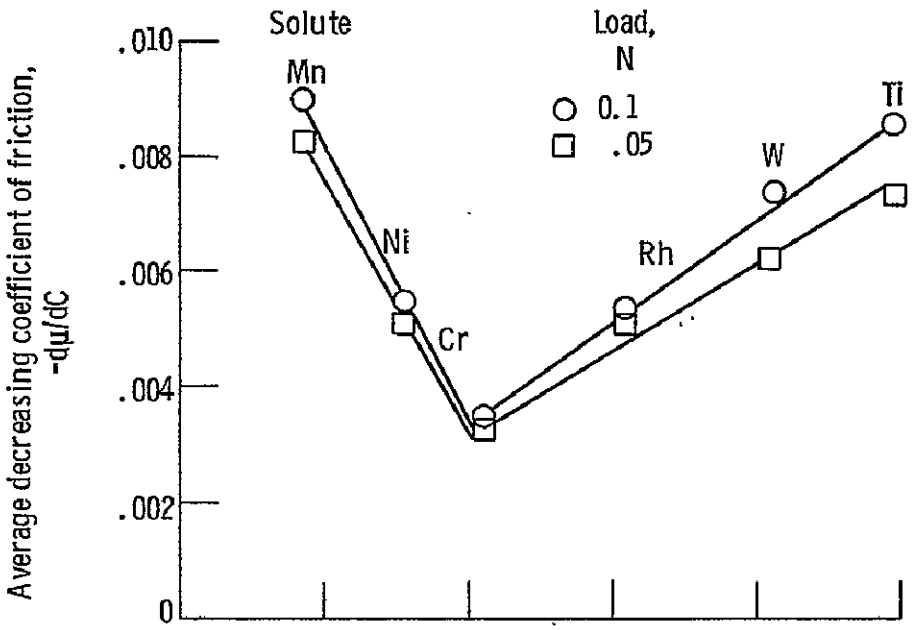

(a) Decreasing rate of change of coefficient of friction.

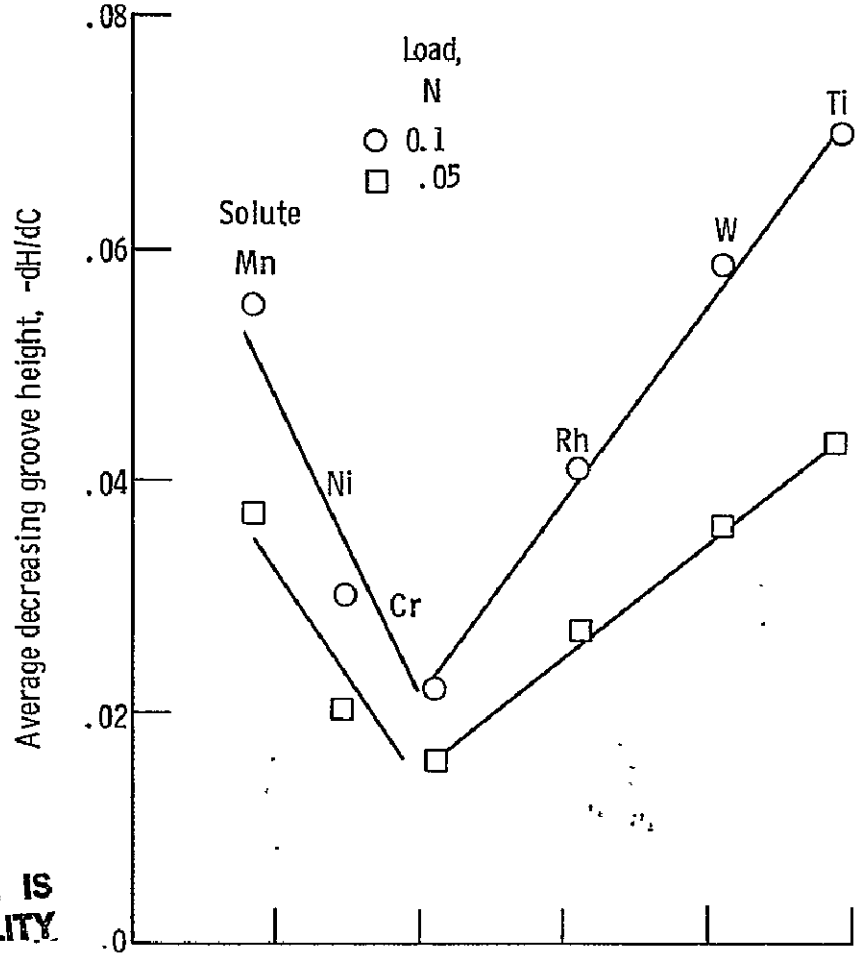

(b) Decreasing rate of change of groove height.

Figure 11. - Rates of change of coefficient of friction, groove height, and contact pressure as function of solute to iron atomic radius ratio.

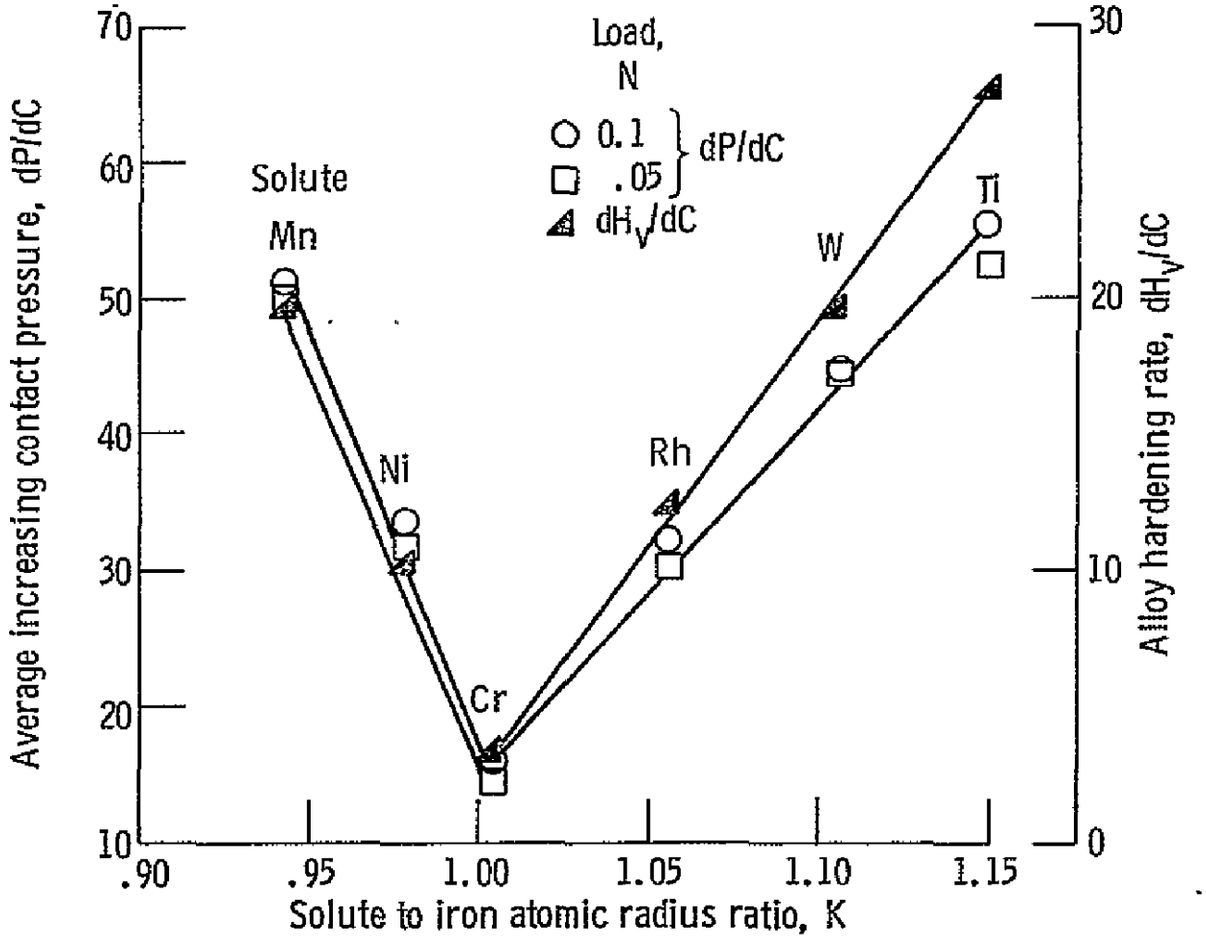

(c) Increasing rate of change of contact pressure.

Figure 11. - Concluded.

National Aeronautics and Space Administration

Washington, D.C.
20546

Official Business
Penalty for Private Use, $300

SPECIAL FOURTH CLASS MAIL
BOOK

Postage and Fees Paid
National Aeronautics and
Space Administration
NASA-451

U.S.MAIL

NASA

POSTMASTER: If Undeliverable (Section 158 Postal Manual) Do Not Return